



Published in final edited form as:

*Sci Transl Med.* 2013 February 13; 5(172): 172ra21. doi:10.1126/scitranslmed.3004925.

## Impairment of BRCA1-related DNA Double Strand Break Repair Leads to Ovarian Aging in Mice and Humans

Shiny Titus<sup>1,\*</sup>, Fang Li<sup>1,\*</sup>, Robert Stobezki<sup>1</sup>, Komala Akula<sup>1</sup>, Evrim Unsal<sup>1,2</sup>, Kyungah Jeong<sup>1</sup>, Maura Dickler<sup>3</sup>, Mark Robson<sup>3</sup>, Fred Moy<sup>1,4</sup>, Sumanta Goswami<sup>5,1</sup>, and Kutluk Oktay<sup>1,6</sup>

<sup>1</sup>Institute for Fertility Preservation and Laboratory of Molecular Reproduction. Departments of Obstetrics & Gynecology, and Cell Biology & Anatomy, New York Medical College, Rye, NY, 10580 and Valhalla, NY 10595, USA

<sup>2</sup>Department of Medical Biology and Genetics, Istanbul Bilim University School of Medicine, Ankara, Turkey

<sup>3</sup>Department of Medicine, Memorial Sloan-Kettering Cancer Center and Weill Medical College of Cornell University, New York, NY 10021, USA

<sup>4</sup>Biometrics, Data Management and PK/PD Unit, Department of Pathology, New York Medical College Valhalla, NY10595, USA

<sup>5</sup>Department of Biology, Yeshiva University, New York, NY10033, USA

<sup>6</sup>Reproductive Specialists of New York, Rye, NY 10580, USA

### Abstract

The underlying mechanism behind age-induced wastage of the human ovarian follicle reserve is unknown. In this study, we identify impaired ATM (ataxia-telangiectasia mutated)-mediated DNA double strand break (DSB) repair as a cause of aging in mouse and human oocytes. We show that DSBs accumulate in primordial follicles with age. In parallel, expression of key DNA DSB repair genes *BRCA1*, *MRE11*, *Rad51*, and *ATM*, but not *BRCA2*, decline in single mouse and human oocytes. In *BRCA1*-deficient mice, reproductive capacity was impaired, primordial follicle counts were lower, and DSBs were increased in remaining follicles with age relative to wild-type mice. Furthermore, oocyte-specific knockdown of *BRCA1*, *MRE11*, *Rad51* and *ATM* expression increased DSBs and reduced survival while *BRCA1* overexpression enhanced both parameters. Likewise, ovarian reserve was impaired in young women with germline *BRCA1* mutations compared to controls as determined by serum concentrations of anti-mullerian hormone. These data implicate DNA DSB repair efficiency as an important determinant of oocyte aging in women.

\*Corresponding author: [koktay@fertilitypreservation.org](mailto:koktay@fertilitypreservation.org).

\*These authors made equal contributions to this work.

**Author contributions:** K.O. conceived the idea and designed and directed the study; S.T., F.L., R.S., K.A., AND E.U. performed the laboratory experiments; K.O., M.D., M.R., and K.J. recruited patients and/or collected/tabulated data for the clinical studies; S.G. developed the single-cell qRT-PCR system and supervised the molecular biology experiments; F.M. reviewed the raw data and performed statistical analysis; K.O. wrote the manuscript.

**Competing Interests:** The authors declare that they have no competing interests.

## INTRODUCTION

Among the major challenges in women's reproductive health are the age-related decline in reproductive performance and a parallel increase in chromosomally abnormal conceptions. The decline in reproductive performance or oocyte quality is closely tied to the decline in ovarian follicular reserve. Human ovarian follicle reserve is established in utero and shows a continuous decline thereafter. Despite the fact that approximately one million oocytes are present at birth in the human ovary, only around 500 of those ovulate during reproductive life, and the remaining 99.9% are wasted [see fig. S1 for a representation of human ovarian follicle development (1)]. The decline in ovarian reserve is nonlinear and seems to accelerate with age (2–4). This leads to near complete exhaustion by the mean age of 51 to 52 years (2). The causes of this high attrition and the mechanism of its acceleration in later reproductive ages are unknown. If this mechanism is identified, then targeted treatment strategies may be developed to improve reproductive performance and delay menopause. Mathematical models suggest that if the depletion of ovarian follicle reserve could be slowed down, menopause could be delayed to age 71 (2).

Cells encounter DNA damage induced by both external and internal factors. Among the various types of DNA damage induced by environmental genotoxins, DNA double-strand breaks (DSBs) are the most deleterious type of damage and can substantially alter genetic integrity. The ataxiatelangiectasia mutated (ATM)-mediated DNA damage-signaling (DDS) pathway regulates the repair of DNA DSBs via a homologous recombination mechanism (fig. S2). For cases in which the DNA damage cannot be repaired, cells are eliminated by apoptotic cell death or undergo senescence—complete withdrawal from the cell cycle—to avoid severe mutagenic consequences (5).

*BRCA1* and *BRCA2* are crucial members of the ATM-mediated DSB repair family of genes, and mutations in the *BRCA* genes are associated with risk of breast, ovarian, and other cancers (6, 7). The *BRCA1* protein functions synergistically with the *RAD51* protein, which performs a key role in homologous recombination during DNA repair and may also regulate mitotic progression in concert with the cell-cycle checkpoint protein kinase *CHK2* (8). The loss of *BRCA1* results in genetic instability, triggering a p53-mediated cell cycle checkpoint (9). Although *BRCA1* is predominantly involved in cell cycle control, and through its association with *Rad51* (10), with homologous recombination repair of DNA DSBs, the biological role of *BRCA2* appears to be confined to homologous recombination (11).

We previously reported that women who carry germline mutations in the *BRCA1* gene show low response to ovarian stimulation while undergoing fertility preservation by oocyte or embryo cryopreservation (12). Recent research also suggests that women with *BRCA1* mutations may experience earlier menopause (13). These observations support the possible role of DNA DSB repair in maintenance of human ovarian reserve and suggest that ovarian reserve is prematurely diminished in women with *BRCA1* mutations.

Chemotherapy exposure induces DSBs in human and rodent oocytes, which triggers a DNA repair response by ATM-mediated DDS pathways, and rodent oocytes possess the capacity to repair DSBs generated by genotoxic stressors (14, 15). Here, we studied the role of

*BRCA1*, *BRCA2*, and associated DSB repair genes in the maintenance of oocyte reserve in human and mouse ovaries. We hypothesized that DNA DSB repair is vital for the maintenance of oocyte reserve and that the decline in its efficiency with age plays a key role in ovarian aging.

## RESULTS

### Increased DSBs in aging mouse and human oocytes

If DNA DSB repair efficiency decreases with age then DNA DSBs should accumulate in oocytes over time. As a first test of this hypothesis, we used Friends leukemia virus B (FVB) mice, which show a significant decline in ovarian reserve between 4 to 5 weeks of age (“young”) and 11 to 12 months of age (“old”). By proportion, 11 to 12 months in FVB mice corresponds to the late third decade of life in women, when oocyte reserve and quality show significant declines (16). We first immunostained ovarian sections from “young” and “old” mice ( $N=8/\text{group}$ ) with an antibody to histone  $\gamma\text{H2AX}$  (anti- $\gamma\text{H2AX}$ ) to determine the extent of DSBs in primordial follicle oocytes. Histone H2AX, one of the several variants of the nucleosome core histone H2A, becomes phosphorylated on serine 139 in response to DSBs ( $\gamma\text{H2AX}$ ). Within seconds of DSB formation,  $\gamma\text{H2AX}$  foci are formed at the site of DNA damage, which can be detected by confocal microscopy or immunohistochemistry to quantify DNA damage. Foci of  $\gamma\text{H2AX}$  represent DSBs in a 1:1 manner, enabling sensitive quantification of DSBs (17).

We found that the percentage of  $\gamma\text{H2AX}$ -positive primordial follicles (see fig. S1 for overview of ovarian follicle stages) increased significantly in the old vs. young mice ( $58.5\% \pm 3.7$  vs.  $32.6\% \pm 2.5$ ,  $P < 0.001$ ; Student’s  $t$  test) (Fig. 1A). In parallel, mean  $\gamma\text{H2AX}$ -foci increased significantly in immature (prophase-I) germinal vesicle (GV)-stage oocytes (18) (fig. S3) obtained from antral follicles of old versus young mice ( $1,297.9 \pm 193$  vs.  $436.2 \pm 64.4$ ,  $P < 0.001$ ; Student’s  $t$  test; Fig. 1B). The percentage of  $\gamma\text{H2AX}$ -positive granulosa cells (somatic cells that surround the oocyte and produce sex hormones; fig. S1) in developing follicles of FVB mice did not show a difference between young and old mice (fig. S4A), indicating the lack of an age-related increase in DSBs in the non-germ cell component of the ovarian follicles.

Similar to mice, DSBs were increased with age in human primordial follicles [ $19.0\% \pm 5.1$  in group  $\leq 14$  years (yrs) vs.  $63.6\% \pm 6.5$  in group  $\geq 21$  yrs,  $P < 0.01$ ; Student’s  $t$  test] (Fig. 1C) and GV oocytes ( $593.8 \pm 181.8$  in group  $\geq 35$  yrs vs.  $55.8 \pm 19.8$  in group  $\leq 28$  yrs of age,  $P < 0.05$ ; Student’s  $t$  test] (Fig. 1D).

### Decreased expression of DNA DSB repair genes in aging mouse oocytes

To determine the underlying reason for the accumulation of DNA-damaged oocytes with age, we subjected individual mouse oocytes to quantitative reverse transcription-polymerase chain reaction (qRT-PCR) (Fig. 2) and found that the expression of *BRCA1* ( $P < 0.01$ ; Student’s  $t$  test) (Fig. 2A), *MRE11* ( $P < 0.001$ ; Student  $t$  test) (Fig. 2C), *Rad51* ( $P < 0.01$ ; Student’s  $t$  test) (Fig. 2D), and *ATM* ( $P < 0.001$ ; Student’s  $t$  test) (Fig. 2E), but not *BRCA2* ( $P = 0.201$ ; Student’s  $t$  test) (Fig. 2B), declined profoundly in old mice compared to the

young. The additional genes were selected on the basis of their association with BRCA function and key roles in the DDS pathway: MRE11 in sensing DNA damage, Rad51 in homologous recombination, and ATM as the orchestrator of the DDS pathway (4, 11, 19). Likewise, we observed a parallel decline in the protein expression patterns of BRCA1, Mre11, Rad51, and ATM, (Fig. 2, F to J) but not BRCA2 (Fig. 2B). These findings suggest that diminished DSB repair in aging oocytes leads to the accumulation of potentially lethal DSBs with age.

### Decline of DSB repair gene expression with age in human oocytes

Next, we analyzed the expression of key DNA DSB repair genes in single human oocytes isolated from 24 individuals. Mean *BRCA1* gene expression showed a significant age-related decline ( $r=0.60$ ;  $P<0.001$  by linear regression analysis and Student's *t* test) (Fig. 3A). Consistent with the anti-mullerian hormone (AMH) data in human *BRCA* mutation carriers (see below), *BRCA2* gene expression did not show a significant correlation with age in the same oocytes ( $r=0.1$ ,  $P=0.75$  by linear regression analysis and Student's *t* test) (Fig. 3B). Furthermore, we observed an age-related decline in expression of *MRE11* ( $r=0.447$ ,  $P<0.03$  by linear regression analysis and Student's *t* test) (Fig. 3C), *Rad51* ( $r=0.5$ ,  $P<0.004$  by linear regression analysis and Student's *t* test) (Fig. 3D), and *ATM* ( $r=0.4$ ,  $P<0.003$  by Linear regression analysis and Student's *t* test) (Fig. 3E) in the same single human oocytes. When we analyzed the regression curves for gene expression changes after the age of 36 years—the time when the oocyte reserve is known to deteriorate in an accelerated fashion in humans (2, 20)—we found that the decline in gene expression was also accelerated for *MRE11* ( $P<0.05$ ; Student's *t* test), *Rad51* ( $P<0.01$ ; Student's *t* test), and *ATM* ( $P<0.05$ ; Student's *t* test), but not for *BRCA1* ( $P=0.8$ ; Student's *t* test) compared to the decline in gene expression levels seen in oocytes isolated from women under age 36 (Fig. 3F). For the same older age group, *BRCA2* gene expression showed a nonsignificant negative trend ( $P=0.08$ ; Student's *t* test) (Fig. 3F).

Confirming the findings from gene expression studies, expression of the BRCA1 protein, but not BRCA2, was also lower in oocytes from older individuals relative to the young. Likewise, the protein expression of corresponding genes was lower in older oocytes (Fig. 3, G to K). These data indicate a relationship between the age-related decline in human oocyte reserve and the function of *BRCA1*, *Rad51*, *MRE11*, and *ATM* but not *BRCA2* in reproductive-age women.

### Diminished reproductive capacity in *BRCA1*-mutant mice

The studies above show a strong relationship among *BRCA1* mRNA expression, DNA DSB repair, and oocyte aging. To further investigate the mechanisms behind this relationship and to determine the impact of BRCA function (and hence the importance of intact DNA DSB repair) on reproductive performance, we studied *BRCA1* mutant mice (heterozygote, *BRCA1*<sup>+/ $\Delta$ 11</sup>) and two versions of *BRCA2* mutant mice (heterozygote, *BRCA2*<sup>+/ $\Delta$ 27</sup> and homozygote, *BRCA2* <sup>$\Delta$ 27/ $\Delta$ 27</sup>). *BRCA1*-deficient homozygous mice were not viable as previously reported (9).

We first confirmed that oocytes from *BRCA1* and *BRCA2* heterozygous mutant mice had lower *BRCA1* and *BRCA2* gene expression relative to wild-type mice (Fig. 4A) and hence were *BRCA1* or *BRCA2* deficient. Likewise, we showed that *BRCA2*<sup>Δ27/Δ27</sup> mouse oocytes did not express exon 27 of the *BRCA2* gene (Fig. 4B). Consistent with our previous data in women (12), we found that *BRCA1*<sup>+Δ11</sup> mice (*N*=3 mice/group) produced fewer oocytes in response to ovarian stimulation compared with wild-type mice (14±7.8 vs. 33.3±0.9; *P*<0.05; Student's *t* test; Fig. 4C) and had smaller litter sizes after mating (5.6±1.5 vs. 7.6±1.4 pups; *P*<0.05; Student's *t* test, *N*=8/group) (Fig. 4E). The total primordial follicle numbers per ovary were lower in both 5-day (2,292.5±163.8 versus 3,108±96.1; *N*=6/group; *P*<0.01, Student's *t* test) (Fig. 4, G, L, and N) and 4-month-old (408.3±63.4 versus 702.9±79.5; *N*=6/group; *P*<0.05, Student's *t* test) (Fig. 4, G and P) *BRCA1*<sup>+Δ11</sup> mice relative to wild-type mice (Fig. 4, K, M, and O). A significantly higher percentage of follicles became γH2AX-positive by 4 months of age in *BRCA1*<sup>+Δ11</sup> mice compared with wild-type mice (75.7±2.7 vs. 58.8±3.6, *N*=6/group; *P*<0.01, Student's *t* test (Fig. 4, I, Q, and R), indicating that the mutant mice had a higher propensity for accumulating DNA damage postnatally as a result of deficient DSB repair. In contrast, *BRCA2*<sup>+Δ27</sup> and *BRCA2*<sup>Δ27/Δ27</sup> mice had similar oocyte yields (Fig. 4D) and litter sizes (Fig. 4F) as wild-type mice. Neither the follicle numbers (Fig. 4H) nor the γH2AX-positivity (Fig. 4J) differed when *BRCA2*<sup>+Δ27</sup> and *BRCA2*<sup>Δ27/Δ27</sup> mice were compared to wild-type mice [by analysis of variance (ANOVA)]. The percentage of γH2AX-positive granulosa cells of developing follicles did not differ between the 4-month-old *BRCA1*<sup>+Δ11</sup> mice and the wild type (fig. S4B).

Together, these data show that the *BRCA1* but not the *BRCA2* gene plays a role in ovarian aging and establish that intact DNA DSB repair is fundamental in the maintenance of oocyte reserve and genomic integrity.

### Impact of *BRCA1* and related genes in the ATM-mediated DDS pathway on oocyte aging

In our next series of experiments, we first showed that oocytes from old mice (11 to 12 months) exposed to genotoxic stress in vitro (H<sub>2</sub>O<sub>2</sub>) had a significantly lower survival compared to oocytes from young mice (3 to 4 weeks) (fig. S5A). These data indicated that aging oocytes indeed have a reduced capacity to repair DNA damage.

To further investigate the acute oocyte-specific functions of *BRCA1* and associated ATM-mediated DDS pathway genes in guarding the oocyte genome and cell survival, we injected young FVB mouse oocytes with *BRCA1*-, *MRE11*-, *RAD51*-, and *ATM*-targeted small interfering RNAs (siRNAs) as well as an “all-star negative control siRNA” as a sham control. The siRNA-treated oocytes were then exposed to H<sub>2</sub>O<sub>2</sub> to induce genotoxic stress. All oocytes with siRNA-downregulated gene expression showed significantly higher mean numbers of γH2AX-positive foci compared to sham siRNA-treated oocytes: siBRCA1 (816±260.16, *P*<0.003; Student's *t* test), siMRE11 (720.6±195.5, *P*<0.04; Student's *t* test), siRad51 (721±238.86, *P*<0.02; Student's *t* test) siATM (541.6±168.3, *P*<0.01; Student's *t* test) all versus scrambled siRNA (268.67±60.79) (Fig. 5A). These findings indicate the importance of acute and active DNA DSB repair in maintaining oocyte genomic integrity.

The same siRNA-downregulated oocytes also showed significantly higher fluorescence intensity of anticaspase 3 (AC-3; an apoptosis marker) after H<sub>2</sub>O<sub>2</sub> treatment: siBRCA1 (102.96±5.46,  $P<0.01$ ; Student's *t* test), siATM (144.8±17.7,  $P<0.001$ ; Student's *t* test), siMRE11 (144.6±10.89,  $P<0.001$ ; Student's *t* test), and siRad51, (165.6±20.68,  $P<0.001$ ; Student's *t* test) all versus scrambled siRNA (65.94±23.85,  $P<0.01$ ; Student's *t* test). These observations indicated that interference with ATM-mediated DNA repair resulted in activation of apoptotic pathways in oocytes (Fig. 5B). After 24 h in culture, those oocytes treated with *BRCA1*, *MRE11*, *RAD51*, or *ATM* siRNAs also exhibited reduced survival compared to the scrambled siRNA-treated oocytes (Fig. 5C) (29.82%, 37.5%, 34.2%, and 44.6% versus 64.81%, respectively  $P<0.05$ ; Fisher's exact test); these findings showed that acute function of the ATM-mediated DNA DSB repair pathway was critical for oocyte survival. Nearly all of the noninjected control oocytes (51 out of 52, 98.07%) survived under the same culture conditions.

Next, to confirm that DNA DSB repair is crucial for oocyte survival, we tested whether *BRCA1* overexpression can increase resistance to genotoxic stress by exposing mock-injected and *BRCA1* cDNA-injected old mouse oocytes to H<sub>2</sub>O<sub>2</sub> and then testing survival rates compared to those of young oocytes. *BRCA1* overexpression resulted in survival rates, in old mouse oocytes after H<sub>2</sub>O<sub>2</sub> treatment, that were comparable to those of young oocytes that had been mock-injected and exposed to genotoxic stress (fig. S5B).

Together, the data described thus far show that intact DNA DSB repair function is acutely essential in maintaining oocyte genomic integrity and survival and that restoration of BRCA1 function may prolong longevity of aging oocytes.

### Lower ovarian reserve in women with BRCA mutations

Next, in an attempt to translate the findings from transgenic mice to women, we assessed the importance of an intact DNA DSB repair function in the maintenance of ovarian reserves in human by taking advantage of an “experiment of nature.” We performed the following series of experiments in a unique population of young women ( $N=84$ ) who had been tested for the presence of *BRCA* mutations.

AMH is a sensitive serum marker that approximates primordial follicle reserve and predicts menopausal age (21). We prospectively compared serum AMH concentrations in women with ( $N=24$ /group, mean age 34.8±4.8 years) (table S3) and without ( $N=60$ /group, mean age 36.3±3.5 years) *BRCA* mutations and found that those who carry mutations displayed significantly lower serum concentrations of AMH (1.22±0.92 ng/mL versus 2.23±1.56,  $P<0.0001$ ; ANOVA) (Fig. 6) even though the mean ages of the two groups were similar.

When we analyzed the impact of mutations in *BRCA1* versus *BRCA2* on ovarian reserve compared to those who tested negative for the same ( $N=60$ /group, mean age 36.3±3.5 years), the significance remained for *BRCA1* mutations [ $N=15$ /group (two patients had both *BRCA1* and *BRCA2* mutations), mean AMH concentrations=1.12±0.73 ng/mL,  $P<0.0001$ ; ANOVA] but not for *BRCA2*-only mutations ( $N=9$ /group, AMH=1.39±1.20,  $P=0.127$ ; ANOVA) (Fig. 6). These data indicate that women with *BRCA1* mutations have diminished ovarian reserve and validate in humans the findings from the transgenic mouse models. The

data are also consistent with lower response to ovarian stimulation (12) and earlier menopausal age (13) shown previously in human *BRCA1*-mutation carriers.

## DISCUSSION

Here, we show that impairment of DNA DSB repair is associated with accelerated loss of ovarian follicular reserve and accumulation of DSBs in human oocytes. Moreover, we demonstrated that the expression of *BRCA1* and other key genes in the ATM-pathway decline with age in human oocytes. This decline mirrors the previously reported age-related diminishment in oocyte reserve (2) and reproductive function (4, 22–24), indicating a relationship between DNA DSB repair and ovarian aging. In a unique setting of women with *BRCA1* mutations and in combination with a *BRCA1*-deficient mouse model as well as by using single-cell qRT-PCR studies, we uncovered a compelling central role for DNA repair efficiency in human ovarian aging. RNA interference experiments showed that acute and active DSB repair was critical for oocyte survival and genomic integrity. The agreement between the mouse and human data pinpoints impaired DNA DSB repair as a universal mechanism of oocyte aging in mammals.

Our findings may also shed light on why there is a significant compromise in reproductive function during the latter half of the third decade of life (24, 25). We found that while *BRCA1* gene expression declined over the ages of 24 to 41 years, this decline showed a sharper downward trend for *ATM*, *Rad51*, and *MRE11* after age 36. It is probable that the sharper decline in DNA DSB repair via homologous recombination leaves oocyte reserves more prone to genotoxicants. This situation, in turn, results in the rapid accumulation of severe DSBs in oocytes, which triggers apoptotic mechanisms and causes the accelerated elimination of oocytes during later reproductive years. Those oocytes that survive despite the accumulation of DNA damage may be functionally impaired, which would explain the decline in reproductive performance during the 10 to 15 years prior to menopause (24, 25).

A careful second look at human diseases of homologous recombination supports our findings and demonstrates a relationship between DNA repair and maintenance of oocyte reserve. For example, both in ataxia telangiectasia mutated syndrome (26) and Fanconi anemia, reproduction is altered as a result of early depletion of oocyte reserves (27). Likewise in Bloom syndrome, in which there is a deficiency of homologous recombination DNA repair, females experience early menopause and infertility (28). Moreover, a recent meta-analysis of GWASs looking at SNPs associated with age at natural menopause also identified a number of DNA repair genes as potential susceptibility genes of menopause (18). Among the genes identified is *UIMC1*, which encodes a protein that physically interacts with the BRCA1 protein and is thought to recruit BRCA1 to sites of DNA damage and to initiate checkpoint control in the G2/M phase of the cell cycle in human and mouse cell lines (29).

The siRNA experiments indicated a broader role, in oocyte aging, for DNA DSB repair via homologous recombination than just the *BRCA1* gene alone, as interference with expression of *BRCA1*, *Rad51*, *MRE11*, or *ATM* resulted in increased DSBs and reduced oocyte survival. Although the products of all three of these genes collaborate with BRCA1 (30),

they are also critical in the main function of ATM-mediated DNA DSB repair pathway. Rad51 is essential in homologous recombination as it is involved in the search for homology and strand-pairing stages of the process (31). MRE11 functions in homologous recombination, meiotic recombination, and telomere maintenance (32). The ATM kinase is a central figure in DSB repair that helps coordinate and integrate repair and checkpoint functions (33). Hence, the knockdown of any of these essential genes would decrease the function of the DSB repair complex, resulting in the accumulation of severe DNA damage, which in turn would trigger cell death mechanisms, explaining reduced oocyte survival.

Although not the focus of this study, we noted  $\gamma$ H2AX staining in some granulosa cells of developing follicles, but this was not affected by aging. The presence of DSBs in granulosa cells can be explained by their high metabolic activity that results from the cells being in active mitosis, which presumably creates an oxygen radical-rich environment. It is possible that one of the key functions of granulosa cells is to shield the oocyte against genotoxic stress. In fact, granulosa cells are endowed with mechanisms to counteract oxidative stress (34). In our previous work, we found that the granulosa cells that are exposed to genotoxic chemotherapy become  $\gamma$ H2AX positive and show ATM activation but not all eventually express AC-3 or become apoptotic (14). This observation indicates that some granulosa cells are able to repair DSBs and survive. Hence the presence of  $\gamma$ H2AX in seemingly healthy granulosa cells may indicate that the ATM-mediated DSB repair pathway is successfully carrying out its functions. These findings stress the need for further research on the role of somatic cells in ovarian aging.

Even though our study points to a broader role of DNA DSB repair via homologous recombination in oocyte aging in humans, it also has immediate clinical implications for *BRCA1*-mutation carriers. Although a retrospective study did not detect a self-reported impairment of fertility in *BRCA*-mutation carriers, it could not rule out the possibility of decline in fertility at later reproductive ages (35, 36). Consistent with this possibility, our data show that *BRCA1*-mutation carriers with a mean age of 36 years have lower ovarian reserves compared to controls as measured by serum AMH concentrations. It is likely that, as the function of the intact *BRCA1* allele and the expression of other ATM-mediated DNA DSB repair genes decline in oocytes significantly during later reproductive years, the *BRCA*-deficiency may become more relevant clinically. This is apparent from the recent reports of earlier menopause (13) and low response to ovarian stimulation after age 33 years (12) in *BRCA1*-mutation carriers. Moreover, because we previously showed that mammalian oocytes are capable of survival by repairing chemotherapy-induced DSBs (37), it is possible that women with deficient *BRCA* function are more likely to lose their ovarian reserves and fertility after cancer treatments.

It is also possible that *BRCA1*-mutation carriers are born with lower ovarian reserves as were newborn *BRCA1* heterozygous mice in our study (Fig. 4, G, I, and N). Given that *BRCA1* also plays a role in both mitotic (8) and meiotic (38) processes, the physiological attrition of oogonia and oocytes may proceed at a higher pace during fetal life when *BRCA1* gene function is deficient. Furthermore, *BRCA1*<sup>+/ $\Delta$ 11</sup> mice demonstrated higher percentages of follicles with DSBs (as shown by  $\gamma$ H2AX expression) at 4 months of life but not at birth



compared to wild type; this implies that impaired DNA DSB repair renders oocytes more prone to DNA damage in postnatal life.

Even though we did not find a clear relationship between *BRCA2* gene function and age in females younger than 41 years of age, this could be because of a subtler decline in *BRCA2* gene function with age compared to *BRCA1*. Supporting this possibility, we observed a trend toward a decline in oocyte *BRCA2* gene expression in women only after 36 years of age. This subtler decline may not result in a clinically significant level of *BRCA2* gene malfunction until past the reproductive age upper limit of 45 to 46 years.

While ovarian reserve and fertility decline with age, pregnancy failures and meiotic errors resulting in chromosomally abnormal conceptions increase in parallel (39). Currently, the mechanism behind this decline in oocyte quality is unknown. Recent research implicated BRCA1 as a key protein in regulating meiotic spindle assembly and spindle assembly checkpoint activation in mouse oocytes (38), and its expression was associated with an age-related increase in aneuploidy in the same species (40). Furthermore, MRE11 is also implicated in efficient chromosome pairing during meiosis in *Tetrahymena* (41). In addition, meiotic crossovers, which are regulated by homologous recombination, may also play a role in meiotic stability, and the frequency of meiotic crossovers (chiasmata) declines with age (39, 42–45).

We propose a model that ties together these prior observations with our current findings and explain age-related decline in oocyte reserve and quality under a single mechanism (fig. S6): As DNA repair efficiency declines with age, DSBs accumulate and an increasing fraction of oocytes are eliminated to prevent propagation of resultant severe mutations. At the same time, aneuploidy increases either because of (i) the declining function of BRCA1 in meiotic spindle assembly or (46) (ii) reduced chiasmata (points of DNA cross overs) frequency or both as the function of ATM-mediated DNA DSB repair pathway genes declines with age. Our model predicts that as the expression of ATM-pathway genes decline faster during the third decade of life, the reduction in oocyte reserve and quality accelerates after that stage. This model is also consistent with the previously proposed connection between telomere shortening and oocyte aging because of the involvement of ATM-mediated DNA DSB repair mechanisms in the maintenance of telomeres (47, 48). Investigation of the epigenetic phenomena that result in the decline of DNA DSB repair with age will likely bring fascinating insight into human reproductive aging. That in turn may lead to future treatments that can enhance or maintain DNA repair efficiency and slow down ovarian aging.

## MATERIALS AND METHODS

The institutional review boards of New York Medical College (NYMC) and Memorial Sloan Kettering Cancer Center (MSKCC) approved the clinical study protocols, and written informed consent was obtained from all participants who took part in the prospective observational study (NCT00520364). The animal studies were carried out at NYMC in strict accordance with the recommendations in the Guide for the Care and Use of Laboratory Animals of the U.S. National Institutes of Health (NIH) and the NYMC Institutional Animal Care and Use Committee. All experiments and analysis were performed in multiple

replicates and in a blinded fashion. At least two blinded independent observers confirmed any quantitative assessment. In addition, all data were reviewed, and all statistical analyses were performed by a biostatistician (F.M.) who was impartial to the study. This ensured that there was no bias involved in the results analyses.

### Recovery of materials

**Human**—GV oocytes (those that are resting in the prophase of first meiotic division) were obtained from females aged 24 to 41 years who had no known cause of ovarian dysfunction and were either undergoing in vitro fertilization (IVF) procedures for male or tubal factor infertility or undergoing oocyte collection for fertility preservation. Oocytes were freed of the cumulus cells by a brief treatment with hyaluronidase (200 IU/ml) in M199 medium at room temperature. The oocytes to be used for RNA extraction were first snap-frozen in PBS, and those to be used for immunofluorescence studies were fixed in 4% paraformaldehyde (PFA). Ovarian tissue was obtained from individuals aged 2 to 28 years who were undergoing ovarian freezing for fertility preservation or biopsies during elective gynecological surgery, as well as from organ donors with no known ovarian conditions.

Sera for anti-müllerian hormone (AMH) analysis were prospectively obtained from individuals aged 18 to 42 years, who were screened for *BRCA* mutations because of breast cancer. AMH analysis was performed by ELISA as described previously (49). The referring medical or surgical oncologists ordered *BRCA* testing on the basis of their clinical assessments; hence, the investigators did not have a role in the *BRCA* testing decision. Of the 28 women with *BRCA* mutations, only those with known clinical significance ( $N=24$ ) were included in the final analysis, although the inclusion of other 4 cases did not affect the final results.

**Mouse**—Prophase-I GV oocytes were retrieved from “young” (4 to 5 weeks) and “old” (11 to 12 months) FVB mice 15 h after injection of PMSG (pregnant mare’s serum gonadotropin, Sigma-Aldrich) (5IU). Cumulus oocyte complexes were recovered from ovaries by repeatedly puncturing the ovaries with fine steel needles. Oocytes were freed of the cumulus cells by a brief treatment with hyaluronidase (200 IU/ml) in M199 medium at room temperature.

The oocytes to be used for RNA extraction were first snap-frozen in PBS, and those to be used for immunofluorescence studies were fixed in 4% PFA.

Ovaries were also extracted from “young” and “old” FVB mice, embedded in paraffin, and serially sectioned for immunohistochemical analysis.

### Immunohistochemistry and immunofluorescence

Immunohistochemistry on ovarian tissue sections from both human and mouse with a Ser139 phosphorylation-specific  $\gamma$ H2AX antibody (IHC-00059; Bethyl Laboratory) was performed using enzymatic diaminobenzidine (DAB) staining. Nuclei were counterstained with hematoxylin. Primordial follicles containing a  $\gamma$ H2AX-positive oocyte were considered to be DNA-damaged.

Immunofluorescence studies on oocytes from humans and mice for  $\gamma$ H2AX, BRCA1, BRCA2, Rad51, Mre11, and ATM proteins were performed as described previously (14) with antibodies to  $\gamma$ H2AX (613402; Biolegend), Brca1 (sc-28234; Santa Cruz), Rad51 (ABE257; Millipore), Mre11 (4895; Cell Signaling), and ATM (ab78; abcam). Apoptotic assessment was performed by antibody staining of the apoptotic AC-3 protein (AF-835, R&D Systems). Stained oocytes were evaluated under a Zeiss LSM 710 confocal microscope.

### Assessment of DNA DSB damage

Extensive nuclear labeling with  $\gamma$ H2AX, especially in the form of characteristic foci, is considered to report the presence of DSBs, which are potentially lethal DNA lesions (14, 50). We assessed age-related increases in DNA damage in oocytes and ovarian tissue sections by detection of histone H2AX phosphorylation on Ser139 (51) using a phospho-specific H2AX antibody (52). In performing H2AX analysis in human ovarian tissue and oocytes, we compared two subject cohorts that were at least 7 years apart in age: 18 to 28 years versus 35 to 42 years in the case of GV oocytes, and 2 to 14 years versus 21 to 28 years in the case of primordial follicles. For the former analyses (GV oocytes)[OK?], the older age range represented a time when reproductive indices decline in an accelerated fashion. For the latter analyses (primordial follicles), to achieve meaningful comparisons, we used only ovarian tissue from females younger than 30 years of age, because the primordial follicle density is insufficient in ovarian biopsies from older women.

**Quantitative analysis of fluorescence images**—The oocytes were scanned with a Zeiss confocal microscope, and *z stacks* were acquired for 2- $\mu$ m sections for each sample. The combined image with maximum intensity signal was then imported to Image J for quantitative analysis. For  $\gamma$ H2AX foci analysis, the nuclear area was captured (as identified by DAPI staining), and then the software was directed to count the foci. Alternately, for intensity calculation of AC3 staining, the whole oocyte was selected and the software was then directed to calculate the mean intensity of AC3 expression for individual oocytes.

### qRT-PCR from single mouse and human oocytes

Single oocytes that were previously snap frozen in phosphate-buffered saline (PBS) were thawed and lysed in cell lysis buffer (9803S; Cell signaling, MA). The lysates of single oocytes were subjected to two rounds of RNA amplification using the Sensation RNA amplification kit (SNSAT12; Genisphere, PA). The amplified RNA was purified using the RNA minieasy kit (74104; Qiagen, MD). The quality and quantity of the RNA was measured using nanodrop 1000 from Thermo scientific, and the integrity of the amplified RNA was measured on an Experion capillary electrophoresis setup (Biorad). Amplified RNA (2  $\mu$ g) from each samples was taken for reverse transcription using dTVN and N9 primers and Superscript III reverse transcriptase, all procured from Invitrogen. The resulting cDNA was used to perform real-time qPCR with Sybr green on an Applied Biosystems realtime PCR machine 7300. In order to determine the relative expression of various genes in the young versus old mice and in human oocytes of varying ages, we used the  $\Delta\Delta$ Ct method, which makes use of the expression of housekeeping genes. All PCR primers were procured from Invitrogen (table S1)

## Genotypic and phenotypic analysis of transgenic mice

*BRCA1* and *BRCA2* transgenic mice were selected based on their sensitivity to genotoxic stress (9, 53) and obtained from U.S. National Institutes of Health (NIH) repository. The mice were kept in a temperature and light-regulated room environment with 12h light: 12h dark cycle and bred in house.

*BRCA1*-mutant mice carried a deletion of 330 bp in intron 10 plus 407 bp in exon 11 of the *BRCA1* gene (*Brca1<sup>+/ $\Delta$ 11</sup>*). Owing to the deletion, the *BRCA1 $\Delta$ 11* gene product is retained in the cytoplasm, which severely compromises its nuclear functions. *BRCA1 $\Delta$ 11/ $\Delta$ 11* mice were not viable and died at E7-8; *Brca $\Delta$ 11/ $\Delta$ 11* embryos exhibited both early post-implantation growth retardation and chromosomal abnormalities (9). Gamma irradiation-induced Rad51 focus formation is impaired in cells in which only *Brca1 $\Delta$ 11* was expressed (54).

*BRCA2*-mutant mice carried a deletion in exon 27 of *BRCA2* gene, which codes for domains that interact with RAD51. This interaction is essential for the homologous recombination repair function of *BRCA2* protein. Hence the deletion in exon 27 results in impaired DNA repair and genetic compromise (53).

**Genotyping**—After weaning, tail and ear biopsies were obtained and DNA was isolated for genotyping using manufacturer's protocol. In short, the biopsies were treated in lysis buffer supplemented with proteinase K (Invitrogen, USA) at 55°C overnight. The following day the DNA was precipitated using equal volumes of isopropanol. The pellet washed in 70% ethanol and air-dried. After reconstitution with adequate amount of nuclease free water (NFW), PCR was performed using gene specific primers (table S2) to identify the genotype.

The primers used for identifying *BRCA1* wild type were B004/B005, which amplifies a 450-bp fragment; and for *BRCA1* heterozygous are B004/B007, which amplifies a 550-bp fragment (9). The primers for *BRCA2* wild type were B016/B017 and for *BRCA2* knockout were B016/B018, which both amplify a 700-bp product (55). Upon completion of the PCR reactions, the products were subjected to electrophoresis on a 2% agarose gel and imaged to determine the genotype.

**Mating**—All female mice were housed with heterozygous male mice (2:1 ratio). The pups were weaned at 3 weeks of age; the litter sizes and gender rates were recorded. Mating frequency of based on presence of vaginal plugs and fecundity rates were similar to wild type mice.

**Histomorphometric analysis of *BRCA* mice**—Ovaries from wild-type, heterozygous and homozygous *BRCA* mice were fixed (10% formalin in PBS), embedded in paraffin, and serially sectioned. The serial sections (6- $\mu$ m) were mounted on Superfrost/plus glass slides and stained with hematoxylin and eosin. The primordial (one layer of flattened granulosa cells) follicles were counted, and total follicle numbers were calculated as previously described (56–58).

## RNA interference

Approximately 5–10  $\mu\text{l}$  of *BRCA1* (50  $\mu\text{M}$ , Qiagen), *MRE11*, *RAD51*, and *ATM* siRNAs (50  $\mu\text{M}$ , Santa Cruz) or *BRCA1* cDNA (1 $\mu\text{g}/\mu\text{L}$ , Qiagen) were microinjected into the cytoplasm of fully grown GV oocytes using an Eppendorf FemtoJet (Eppendorf AG, Hamburg, Germany) with observation under a Leica inverted microscope (M50, Kramer Scientific, Amesbury, MA) equipped with an Eppendorf transferman NK2 micromanipulator. After injection, the oocytes were cultured in HTF medium with 0.4% BSA for 8 hours followed by treatment with 250  $\mu\text{M}$   $\text{H}_2\text{O}_2$  for 5 min at 4°C, and the oocytes were then washed in fresh HTF medium three times for 2 min each. The oocytes were then transferred to fresh HTF medium and cultured under paraffin oil at 37°C in an atmosphere of 5%  $\text{CO}_2$  in air. The control oocytes were microinjected with 5 to 10  $\mu\text{l}$  of “All-star negative siRNA” from Qiagen at the concentration of 50  $\mu\text{M}$  following the manufacturer’s protocol. Each experiment was replicated 3 times. Oocyte survival was determined by previously published morphological criteria (59). The surviving oocytes were then subjected to  $\gamma\text{H2AX}$  and AC-3 staining and were analyzed by confocal microscopy as described above.

## Statistical analyses

SPSS 17 for Windows package (SPSS Inc., Chicago, IL) was used for statistical analysis. To choose the appropriate statistical test, Levene’s test of homogeneity of variances ( $P < 0.01$ ) and Kolmogorov-Smirnov test of normality ( $P < 0.01$ ) were performed. Continuous data (presented as mean  $\pm$  SEM) were analyzed by student *t* test and one-way ANOVA followed by the least significant difference (LSD) post hoc test. To analyze the relation between two categorical variables, Fisher’s exact test was performed. The difference was considered statistically significant if the *P* value was less than 0.05. All analyses were two-tailed.

## Supplementary Material

Refer to Web version on PubMed Central for supplementary material.

## Acknowledgments

The authors wish to acknowledge Justin Bral for technical help and Yeshiva University’s postbac fellowship funding for his support. We also would like to thank the entire New York Organ Donor Network staff including its Medical Director Michael J. Goldstein and Harvey Lerner as well as the family members and friends of organ donors.

**Funding:** NIH Grants R01 HDO53112 and R21 HDO61259 from NICHD and NCI to KO support this work.

## REFERENCES AND NOTES

1. Oktay K, Briggs D, Gosden RG. Ontogeny of follicle-stimulating hormone receptor gene expression in isolated human ovarian follicles. *J Clin Endocrinol Metab.* 1997; 82:3748–3751. [PubMed: 9360535]
2. Faddy MJ, Gosden RG, Gougeon A, Richardson SJ, Nelson JF. Accelerated disappearance of ovarian follicles in mid-life: Implications for forecasting menopause. *Hum Reprod.* 1992; 7:1342–1346. [PubMed: 1291557]
3. Younis JS. Ovarian aging: latest thoughts on assessment and management. *Curr Opin Obstet Gynecol.* 2011; 23:427–434. [PubMed: 21897233]

4. Hansen KR, Knowlton NS, Thyer AC, Charleston JS, Soules MR, Klein NA. A new model of reproductive aging: the decline in ovarian non-growing follicle number from birth to menopause. *Hum Reprod.* 2008; 23:699–708. [PubMed: 18192670]
5. Jazayeri A, Falck J, Lukas C, Bartek J, Smith GC, Lukas J, Jackson SP. ATM- and cell cycle-dependent regulation of ATR in response to DNA double-strand breaks. *Nat Cell Biol.* 2006; 8:37–45. [PubMed: 16327781]
6. Robson M, Gilewski T, Haas B, Levin D, Borgen P, Rajan P, Hirschaut Y, Pressman P, Rosen PP, Lesser ML, Norton L, Offit K. BRCA-associated breast cancer in young women. *J Clin Oncol.* 1998; 16:1642–1649. [PubMed: 9586873]
7. Kauff ND, Satagopan JM, Robson ME, Scheuer L, Hensley M, Hudis CA, Ellis NA, Boyd J, Borgen PI, Barakat RR, Norton L, Castiel M, Nafa K, Offit K. Risk-reducing salpingo-oophorectomy in women with a BRCA1 or BRCA2 mutation. *N Engl J Med.* 2002; 346:1609–1615. [PubMed: 12023992]
8. Stolz A, Ertych N, Kienitz A, Vogel C, Schneider V, Fritz B, Jacob R, Dittmar G, Weichert W, Petersen I, Bastians H. The CHK2-BRCA1 tumour suppressor pathway ensures chromosomal stability in human somatic cells. *Nat Cell Biol.* 2010; 12:492–499. [PubMed: 20364141]
9. Shen SX, Weaver Z, Xu X, Li C, Weinstein M, Chen L, Guan XY, Ried T, Deng CX. A targeted disruption of the murine *Brcal* gene causes gamma-irradiation hypersensitivity and genetic instability. *Oncogene.* 1998; 17:3115–3124. [PubMed: 9872327]
10. Scully R, Chen J, Plug A, Xiao Y, Weaver D, Feunteun J, Ashley T, Livingston DM. Association of BRCA1 with Rad51 in mitotic and meiotic cells. *Cell.* 1997; 88:265–275. [PubMed: 9008167]
11. Jackson SP, Bartek J. The DNA-damage response in human biology and disease. *Nature.* 2009; 461:1071–1078. [PubMed: 19847258]
12. Oktay K, Kim JY, Barad D, Babayev SN. Association of BRCA1 mutations with occult primary ovarian insufficiency: a possible explanation for the link between infertility and breast/ovarian cancer risks. *J Clin Oncol.* 2010; 28:240–244. [PubMed: 19996028]
13. Rzepka-Gorska I, Tarnowski B, Chudecka-Glaz A, Gorski B, Zielinska D, Toloczko-Grabarek A. Premature menopause in patients with BRCA1 gene mutation. *Breast Cancer Res Treat.* 2006; 100:59–63. [PubMed: 16773440]
14. Soleimani R, Heytens E, Darzynkiewicz Z, Oktay K. Mechanisms of chemotherapy-induced human ovarian aging: double strand DNA breaks and microvascular compromise. *Aging.* 2011; 3:782–793. [PubMed: 21869459]
15. Kujjo LL, Laine T, Pereira RJ, Kagawa W, Kurumizaka H, Yokoyama S, Perez GI. Enhancing survival of mouse oocytes following chemotherapy or aging by targeting Bax and Rad51. *PLoS One.* 2010; 5:e9204. [PubMed: 20169201]
16. Fox, JG. American College of Laboratory Animal Medicine series. 2. Elsevier; AP, Amsterdam ; Boston: 2007. The mouse in biomedical research. pp. v. <2-4>
17. Lowndes NF, Toh GW. DNA repair: the importance of phosphorylating histone H2AX. *Curr Biol.* 2005; 15:R99–R102. [PubMed: 15694301]
18. Stolk L, Perry JR, Chasman DI, He C, Mangino M, Sulem P, Barbalic M, Broer L, Byrne EM, Ernst F, Esko T, Franceschini N, Gudbjartsson DF, Hottenga JJ, Kraft P, McArdle PF, Porcu E, Shin SY, Smith AV, van Wingerden S, Zhai G, Zhuang WV, Albrecht E, Alizadeh BZ, Aspelund T, Bandinelli S, Lauc LB, Beckmann JS, Boban M, Boerwinkle E, Broekmans FJ, Burri A, Campbell H, Chanock SJ, Chen C, Cornelis MC, Corre T, Coviello AD, d'Adamo P, Davies G, de Faire U, de Geus EJ, Deary IJ, Dedoussis GV, Deloukas P, Ebrahim S, Eiriksdottir G, Emilsson V, Eriksson JG, Fauser BC, Ferrelli L, Ferrucci L, Fischer K, Folsom AR, Garcia ME, Gasparini P, Gieger C, Glazer N, Grobbee DE, Hall P, Haller T, Hankinson SE, Hass M, Hayward C, Heath AC, Hofman A, Ingelsson E, Janssens AC, Johnson AD, Karasik D, Kardia SL, Keyzer J, Kiel DP, Kolcic I, Kutalik Z, Lahti J, Lai S, Laisk T, Laven JS, Lawlor DA, Liu J, Lopez LM, Louwers YV, Magnusson PK, Marongiu M, Martin NG, Klaric IM, Masciullo C, McKnight B, Medland SE, Melzer D, Mooser V, Navarro P, Newman AB, Nyholt DR, Onland-Moret NC, Palotie A, Pare G, Parker AN, Pedersen NL, Peeters PH, Pistis G, Plump AS, Polasek O, Pop VJ, Psaty BM, Raikonen K, Rehnberg E, Rotter JI, Rudan I, Sala C, Salumets A, Scuteri A, Singleton A, Smith JA, Snieder H, Soranzo N, Stacey SN, Starr JM, Stathopoulou MG, Stirrups K, Stolk RP, Stykarsdottir U, Sun YV, Tenesa A, Thorand B, Toniolo D, Tryggvadottir L, Tsui K, Ulivi S, van

- Dam RM, van der Schouw YT, van Gils CH, van Nierop P, Vink JM, Visscher PM, Voorhuis M, Waeber G, Wallaschofski H, Wichmann HE, Widen E, Wijnands-van Gent CJ, Willemsen G, Wilson JF, Wolffenbuttel BH, Wright AF, Yerges-Armstrong LM, Zemunik T, Zgaga L, Zillikens MC, Zygmunt M, Study TL, Arnold AM, Boomsma DI, Buring JE, Crisponi L, Demerath EW, Gudnason V, Harris TB, Hu FB, Hunter DJ, Launer LJ, Metspalu A, Montgomery GW, Oostra BA, Ridker PM, Sanna S, Schlessinger D, Spector TD, Stefansson K, Streeten EA, Thorsteinsdottir U, Uda M, Uitterlinden AG, van Duijn CM, Volzke H, Murray A, Murabito JM, Visser JA, Lunetta KL. Meta-analyses identify 13 loci associated with age at menopause and highlight DNA repair and immune pathways. *Nat Genet.* 2012; 44:260–268. [PubMed: 22267201]
19. Klein HL. The consequences of Rad51 overexpression for normal and tumor cells. *DNA Repair (Amst).* 2008; 7:686–693. [PubMed: 18243065]
  20. Faddy MJ, Gosden RG, Oktay K, Nelson JF. Factoring in complexity and oocyte memory--can transformations and cyperpathology distort reality? *Fertil Steril.* 1999; 71:1170–1172. [PubMed: 10360935]
  21. Broer SL, Eijkemans MJ, Scheffer GJ, van Rooij IA, de Vet A, Themmen AP, Laven JS, de Jong FH, Te Velde ER, Fauser BC, Broekmans FJ. Anti-mullerian hormone predicts menopause: A long-term follow-up study in normoovulatory women. *J Clin Endocrinol Metab.* 2011; 96:2532–2539. [PubMed: 21613357]
  22. Leridon H. Can assisted reproduction technology compensate for the natural decline in fertility with age? A model assessment. *Hum Reprod.* 2004; 19:1548–1553. [PubMed: 15205397]
  23. Marinakis G, Nikolaou D. What is the role of assisted reproduction technology in the management of age-related infertility? *Hum Fertil (Camb).* 2011; 14:8–15. [PubMed: 21329469]
  24. Menken J, Trussell J, Larsen U. Age and infertility. *Science.* 1986; 233:1389–1394. [PubMed: 3755843]
  25. Pellestor F, Andreo B, Arnal F, Humeau C, Demaille J. Maternal aging and chromosomal abnormalities: new data drawn from in vitro unfertilized human oocytes. *Hum Genet.* 2003; 112:195–203. [PubMed: 12522562]
  26. Uhrhammer N, Bay JO, Bignon YJ. Seventh International Workshop on Ataxia-Telangiectasia. *Cancer Res.* 1998; 58:3480–3485. [PubMed: 9699683]
  27. Taniguchi T, D'Andrea AD. Molecular pathogenesis of Fanconi anemia: Recent progress. *Blood.* 2006; 107:4223–4233. [PubMed: 16493006]
  28. Thompson LH, Schild D. Recombinational DNA repair and human disease. *Mutat Res.* 2002; 509:49–78. [PubMed: 12427531]
  29. Wu J, Huen MS, Lu LY, Ye L, Dou Y, Ljungman M, Chen J, Yu X. Histone ubiquitination associates with BRCA1-dependent DNA damage response. *Mol Cell Biol.* 2009; 29:849–860. [PubMed: 19015238]
  30. Wang Y, Cortez D, Yazdi P, Neff N, Elledge SJ, Qin J. BASC a super complex of BRCA1-associated proteins involved in the recognition and repair of aberrant DNA structures. *Genes Dev.* 2000; 14:927–939. [PubMed: 10783165]
  31. Sigurdsson S, Van Komen S, Petukhova G, Sung P. Homologous DNA pairing by human recombination factors Rad51 and Rad54. *J Biol Chem.* 2002; 277:42790–42794. [PubMed: 12205100]
  32. Zhong Q, Chen CF, Li S, Chen Y, Wang CC, Xiao J, Chen PL, Sharp ZD, Lee WH. Association of BRCA1 with the hRad50-hMre11-p95 complex and the DNA damage response. *Science.* 1999; 285:747–750. [PubMed: 10426999]
  33. Derheimer FA, Kastan MB. Multiple roles of ATM in monitoring and maintaining DNA integrity. *FEBS Lett.* 2010; 584:3675–3681. [PubMed: 20580718]
  34. Devine PJ, Perreault SD, Luderer U. Roles of reactive oxygen species and antioxidants in ovarian toxicity. *Biol Reprod.* 2012; 86:27. [PubMed: 22034525]
  35. Pal T, Keefe D, Sun P, Narod SA. Fertility in women with BRCA mutations: a case-control study. *Fertil Steril.* 2010; 93:1805–1808. [PubMed: 19200971]
  36. Lin W, Beattie M, Chen LM, Oktay K, Crawford S, Gold E, Cedars M, Rosen M. Comparison of age at natural menopause in BRCA1/2 mutation carriers to a non-clinic-based sample of women in northern California. *Cancer.* 2013 In press.

37. Soleimani R, Heytens E, Darzynkiewicz Z, Oktay K. Mechanisms of chemotherapy-induced human ovarian aging: double strand DNA breaks and microvascular compromise. *Aging* (Albany NY). 2011; 3:782–793. [PubMed: 21869459]
38. Xiong B, Li S, Ai JS, Yin S, Ouyang YC, Sun SC, Chen DY, Sun QY. BRCA1 is required for meiotic spindle assembly and spindle assembly checkpoint activation in mouse oocytes. *Biol Reprod*. 2008; 79:718–726. [PubMed: 18596218]
39. Jones KT. Meiosis in oocytes: predisposition to aneuploidy and its increased incidence with age. *Hum Reprod Update*. 2008; 14:143–158. [PubMed: 18084010]
40. Pan H, Ma P, Zhu W, Schultz RM. Age-associated increase in aneuploidy and changes in gene expression in mouse eggs. *Dev Biol*. 2008; 316:397–407. [PubMed: 18342300]
41. Lukaszewicz A, Howard-Till RA, Novatchkova M, Mochizuki K, Loidl J. MRE11 and COM1/SAE2 are required for double-strand break repair and efficient chromosome pairing during meiosis of the protist *Tetrahymena*. *Chromosoma*. 2010; 119:505–518. [PubMed: 20422424]
42. Shinohara M, Gasior SL, Bishop DK, Shinohara A. Tid1/Rdh54 promotes colocalization of rad51 and dmc1 during meiotic recombination. *Proc Natl Acad Sci U S A*. 2000; 97:10814–10819. [PubMed: 11005857]
43. Champion MD, Hawley RS. Playing for half the deck: the molecular biology of meiosis. *Nat Cell Biol*. 2002; 4 Suppl:s50–56. [PubMed: 12479615]
44. Watrin E, Peters JM. Cohesin and DNA damage repair. *Exp Cell Res*. 2006; 312:2687–2693. [PubMed: 16876157]
45. Henderson SA, Edwards RG. Chiasma frequency and maternal age in mammals. *Nature*. 1968; 218:22–28. [PubMed: 4230650]
46. Tronov VA, Loginova M, Kramarenko. Methylnitrosourea as challenge mutagen in assessment of the DNA mismatch repair (MMR) activity: association with some types of cancer. *Genetika*. 2008; 44:686–692. [PubMed: 18672802]
47. Keefe DL, Liu L. Telomeres and reproductive aging. *Reprod Fertil Dev*. 2009; 21:10–14. [PubMed: 19152740]
48. McPherson JP, Hande MP, Poonepalli A, Lemmers B, Zablocki E, Migon E, Shehabeldin A, Porras A, Karaskova J, Vukovic B, Squire J, Hakem R. A role for Brca1 in chromosome end maintenance. *Hum Mol Genet*. 2006; 15:831–838. [PubMed: 16446310]
49. Lee S, Ozkavukcu S, Heytens E, Moy F, Alappat RM, Oktay K. Anti-Mullerian hormone and antral follicle count as predictors for embryo/oocyte cryopreservation cycle outcomes in breast cancer patients stimulated with letrozole and follicle stimulating hormone. *J Assist Reprod Genet*. 2011; 28:651–656. [PubMed: 21573682]
50. Rogakou EP, Pilch DR, Orr AH, Ivanova VS, Bonner WM. DNA double-stranded breaks induce histone H2AX phosphorylation on serine 139. *J Biol Chem*. 1998; 273:5858–5868. [PubMed: 9488723]
51. Sedelnikova OA, Rogakou EP, Panyutin IG, Bonner WM. Quantitative detection of (125)IdU-induced DNA double-strand breaks with gamma-H2AX antibody. *Radiat Res*. 2002; 158:486–492. [PubMed: 12236816]
52. Bakkenist CJ, Kastan MB. Initiating cellular stress responses. *Cell*. 2004; 118:9–17. [PubMed: 15242640]
53. Donoho G, Brenneman MA, Cui TX, Donoviel D, Vogel H, Goodwin EH, Chen DJ, Hasty P. Deletion of Brca2 exon 27 causes hypersensitivity to DNA crosslinks, chromosomal instability, and reduced life span in mice. *Genes Chromosomes Cancer*. 2003; 36:317–331. [PubMed: 12619154]
54. Huber LJ, Yang TW, Sarkisian CJ, Master SR, Deng CX, Chodosh LA. Impaired DNA damage response in cells expressing an exon 11-deleted murine Brca1 variant that localizes to nuclear foci. *Mol Cell Biol*. 2001; 21:4005–4015. [PubMed: 11359908]
55. McAllister KA, Bennett LM, Houle CD, Ward T, Malphurs J, Collins NK, Cachafeiro C, Haseman J, Goulding EH, Bunch D, Eddy EM, Davis BJ, Wiseman RW. Cancer susceptibility of mice with a homozygous deletion in the COOH-terminal domain of the Brca2 gene. *Cancer Res*. 2002; 62:990–994. [PubMed: 11861370]



56. Oktay K, Karlikaya G, Akman O, Ojakian GK, Oktay M. Interaction of extracellular matrix and activin-A in the initiation of follicle growth in the mouse ovary. *Biol Reprod.* 2000; 63:457–461. [PubMed: 10906050]
57. Tilly JL. Ovarian follicle counts--not as simple as 1, 2, 3. *Reprod Biol Endocrinol.* 2003; 1:11. [PubMed: 12646064]
58. Ting AY, Petroff BK. Tamoxifen decreases ovarian follicular loss from experimental toxicant DMBA and chemotherapy agents cyclophosphamide and doxorubicin in the rat. *J Assist Reprod Genet.* 2010; 27:591–597. [PubMed: 20711751]
59. Perez GI, Tao XJ, Tilly JL. Fragmentation and death (a.k.a. apoptosis) of ovulated oocytes. *Mol Hum Reprod.* 1999; 5:414–420. [PubMed: 10338364]

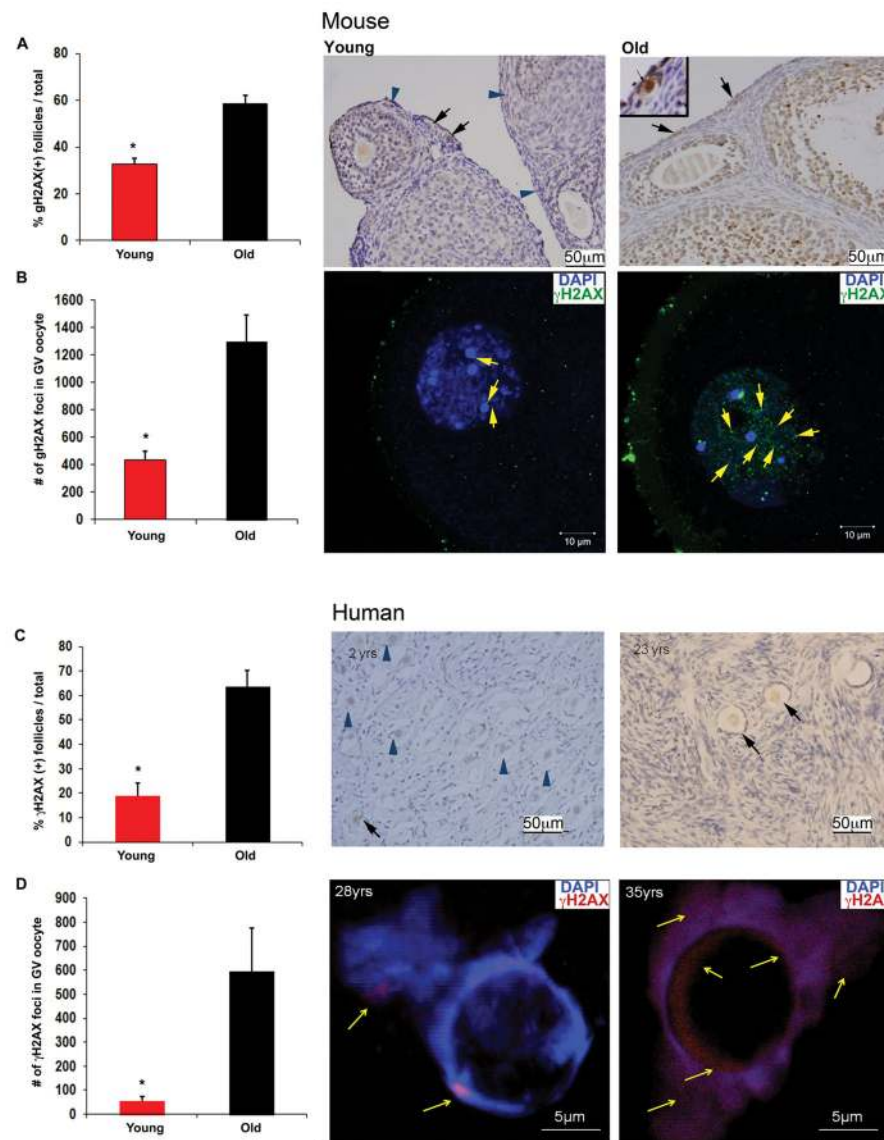


**Fig. 1. Aging-related DSBs in GV oocytes and ovarian tissue from young and old mice and humans**

(A) Bar graphs show a higher percentage of  $\gamma$ H2AX-positive follicles in old (11 to 12 months) compared to young (4 to 5 weeks) mice,  $N=8$ /group;  $*P<0.01$ ; Student's  $t$  test. Adjacent photomicrographs represent  $\gamma$ H2AX staining of young and old FVB mice ovarian sections; Inset (upper left corner of old mice ovarian tissue) shows a higher magnification of the right  $\gamma$ H2AX(+) primordial follicle surrounded by  $\gamma$ H2AX(-) stromal cells in old ovarian tissue. (B) Bar graphs show a higher number of  $\gamma$ H2AX-positive foci per oocyte in old compared to young mice,  $N=13$ /group;  $*P<0.05$ ; Student's  $t$  test. Adjacent photomicrographs represent  $\gamma$ H2AX (green) staining and counter staining of DAPI of young and old FVB mice oocytes. (C) Bar graph shows higher percentage of  $\gamma$ H2AX-positive follicles in age group  $>20$  yrs ( $N=4$ /group, age range 21 to 28yrs) compared to age group  $\leq 20$ yrs ( $N=3$ /group, age range 2 to 14yrs;  $*P<0.01$ ; Student's  $t$  test). Adjacent

photomicrographs represent  $\gamma$ H2AX staining of human ovarian sections in two different age groups. (D) Bar graphs show higher numbers of  $\gamma$ H2AX-positive foci per oocyte in human women age group  $\geq 30$  yrs ( $N=4$ /group, age range 35 to 42yrs) compared to age group  $<30$ yrs ( $N=5$ , age range 23 to 28yrs;  $*P<0.05$ ; Student's  $t$  test). Adjacent photomicrographs represent  $\gamma$ H2AX (red) staining and counter staining for 4',6-diamidino-2-phenylindole, dihydrochloride (DAPI) in human oocytes. Blue arrow head:  $\gamma$ H2AX-negative follicle; black arrow:  $\gamma$ H2AX-positive follicle; yellow arrow:  $\gamma$ H2AX foci. All bar graphs show the mean  $\pm$  standard error of the mean (S.E.M.).

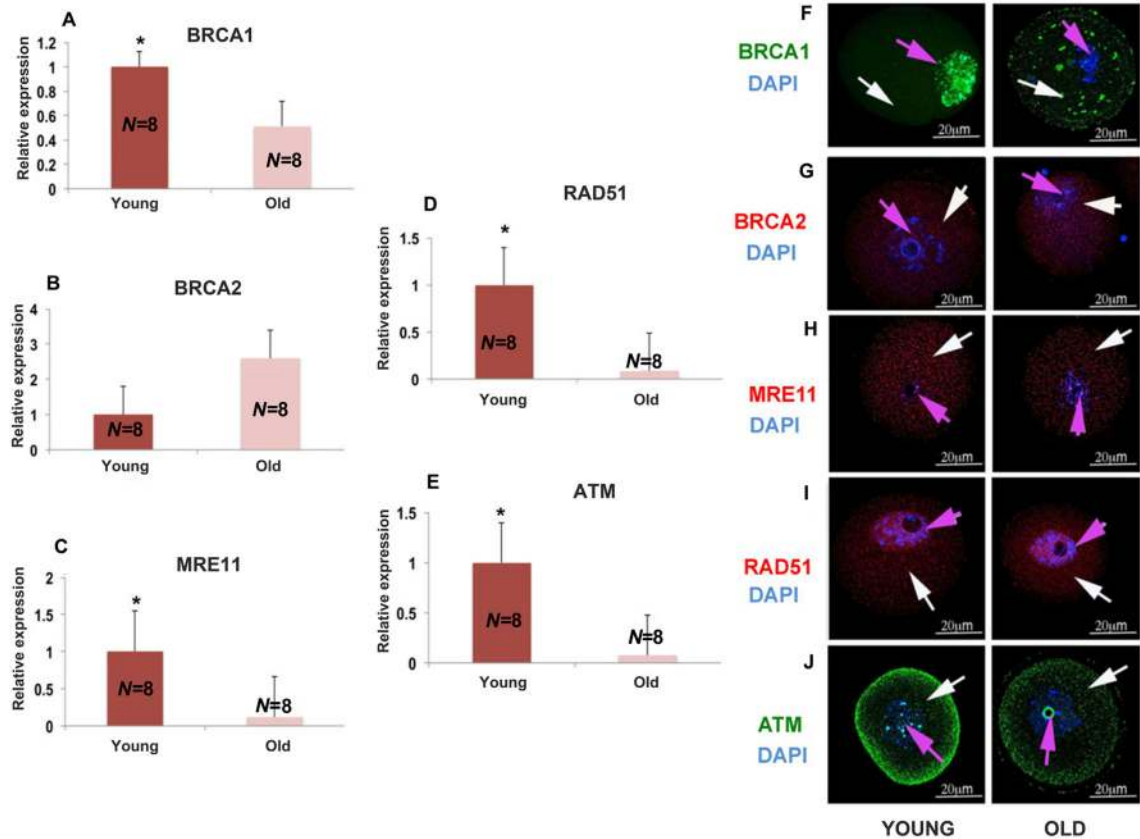


### Fig. 2. Expression of DNA repair genes and proteins in mouse oocytes

Significant decrease in the expression of DNA repair genes in old mice (11 to 12 months) compared to young mice (4 to 5 weeks) shown by real time PCR. All results are mean  $\pm$  S.E.M.,  $N=8$ /group. Bar graphs represent the gene expressions and photomicrographs represent the protein expressions. The bar graphs show significantly lower levels of expression for (A) *BRCA1*, (C) *MRE11*, (D) *RAD51*, and (E) *ATM* in old mice compared to young mice (\*\* $P<0.001$ ; Student's *t* test). (B) Shows a nonsignificant change in *BRCA2* expression levels in old mice compared to young mice ( $P=0.2$ ; Student's *t* test). The representative photomicrographs show lower amounts of (F) BRCA1 (green), (H) MRE11 (red), (I) RAD51 (red), and (J) ATM (green) protein expression in old mice compared to young mice. Oocytes were counterstained with DAPI (blue). (G) No significant difference was detected in BRCA2 protein expression patterns in young and old mice. White arrow points to the cytoplasm and pink arrow to the nucleus. All bar graphs show the mean  $\pm$  S.E.M.

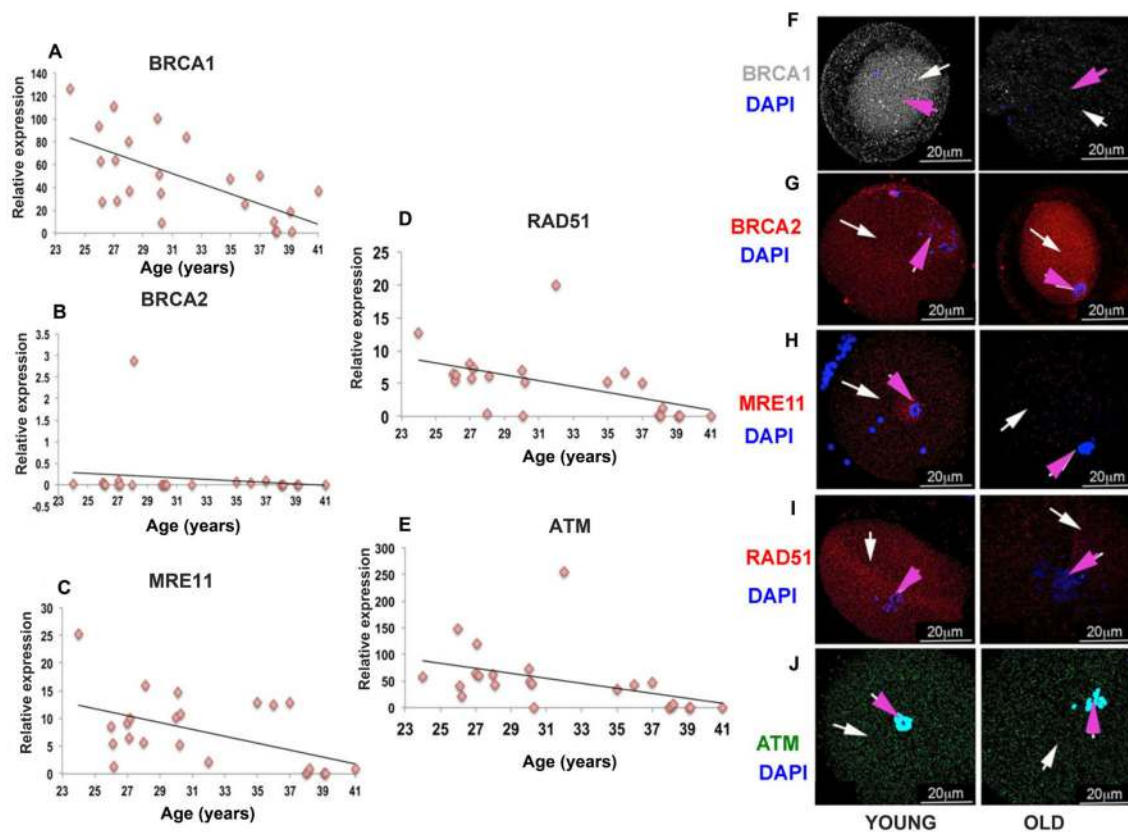


**Fig. 3. Expression of DNA repair genes and proteins in human oocytes**

Scatter plots represent the relative expression of DNA repair genes assessed by qRT-PCR in human oocytes from 24 patients aged 24 to 41 years, some of which show significant age-related declines. Relative expression is defined as. (A) *BRCA1* ( $r=0.60$ ,  $P<0.001$ ; linear regression analysis and Student's *t* test); (C) *MRE11* ( $r=0.447$ ,  $P<0.05$ ; linear regression analysis and Student's *t* test); (D) *RAD51* ( $r=0.5$ ,  $P<0.01$ ; linear regression analysis and Student's *t* test); (E) *ATM* ( $r=0.4$ ,  $P<0.01$ ; linear regression analysis and Student's *t* test) show a decrease in the expression in old compared to young human oocytes. (B) *BRCA2* does not show any significant change in the expression levels as the age progresses ( $r=0.1$ ,  $P=0.75$ ; linear regression analysis and Student's *t* test). Photomicrographs represent the protein expression in human oocytes grouped as old ( $\geq 35$  yrs), young ( $\leq 27$  yrs) and all results are mean  $\pm$  s.e.m. ( $N=4$ /group). Representative photomicrographs (F) *BRCA1* (grey), (H) *MRE11* (red), (I) *RAD51* (red), and (J) *ATM* (green) show decreased protein expression in old (36 to 41 yrs) compared to young (24 to 35 yrs) human oocytes. (G) No decline in expression of *BRCA2* protein (red) was observed in old compared to young human oocytes. White arrow points to cytoplasm and pink arrow to the nucleus. Oocytes were counterstained with DAPI (blue).

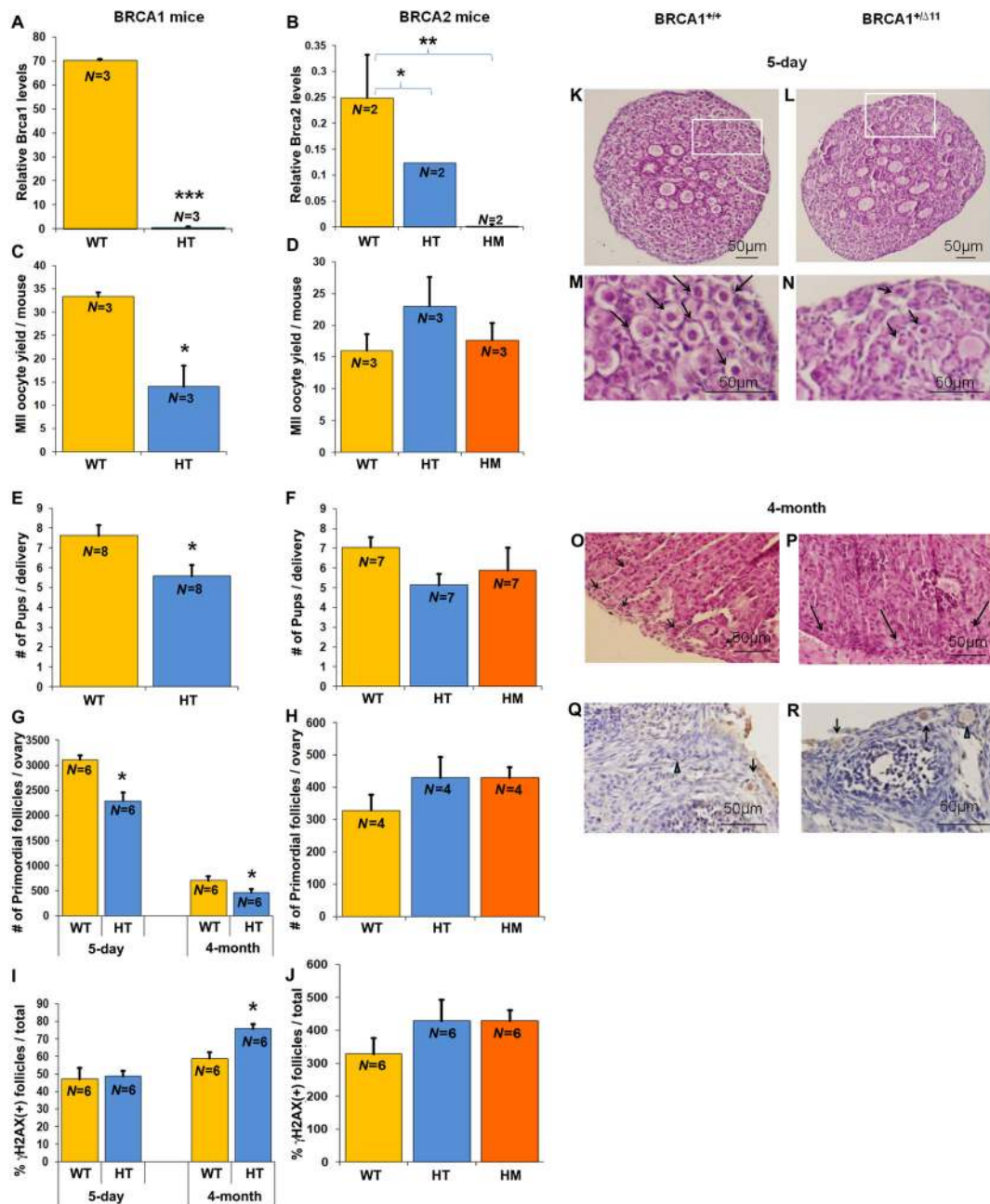


**Fig. 4. BRCA-mutant mouse ovarian function**

(A, B) Relative *BRCA* gene expression levels in *BRCA*-mutant mice. We observed significant *BRCA*-deficiency in heterozygous *BRCA1*<sup>+/ $\Delta$ 11</sup> and *BRCA2*<sup>+/ $\Delta$ 27</sup> mutant mice and the absence of *BRCA* gene expression in *BRCA2* <sup>$\Delta$ 27/ $\Delta$ 27</sup> homozygous mice (HM) compared with wild-type mice (WT) (\*\*\*  $P < 0.0001$  by Student's *t* test, \*\*  $P < 0.001$  by ANOVA, \*  $P < 0.05$  by ANOVA). *BRCA1* HT mice also showed significantly lower MII oocyte yield per female (C) (\*  $P < 0.01$ ; Student's *t* test), (E) reduced litter size (\*  $P < 0.05$ ; Student's *t* test), reduced primordial follicles per ovary (G, L for 5-day ovary, P for 4-month ovary; \*  $P < 0.05$ ; Student's *t* test), and a higher percentage of  $\gamma$ H2AX-positive follicles (I,

**R**, only in 4-month-old mice, \*  $P < 0.01$ ; Student's  $t$  test) versus *BRCA1* wild-type mice (**K**, **O**, and **Q**). No difference was observed for the same comparisons for *BRCA2* HT or HM mice with WT (**D**, **F**, **H**, and **J**, analyzed by ANOVA). Panels **M** and **N** are enlarged views of **K** and **L**, respectively. Black arrows in panels **K**, **L**, **M**, **N**, **O**, and **P** point to primordial follicles; black arrows in **Q** and **R** point to  $\gamma$ H2AX (+) primordial follicles, and blue arrowheads in **Q** and **R** point to  $\gamma$ H2AX (-) primordial follicles. All bar graphs show the mean  $\pm$  S.E.M.

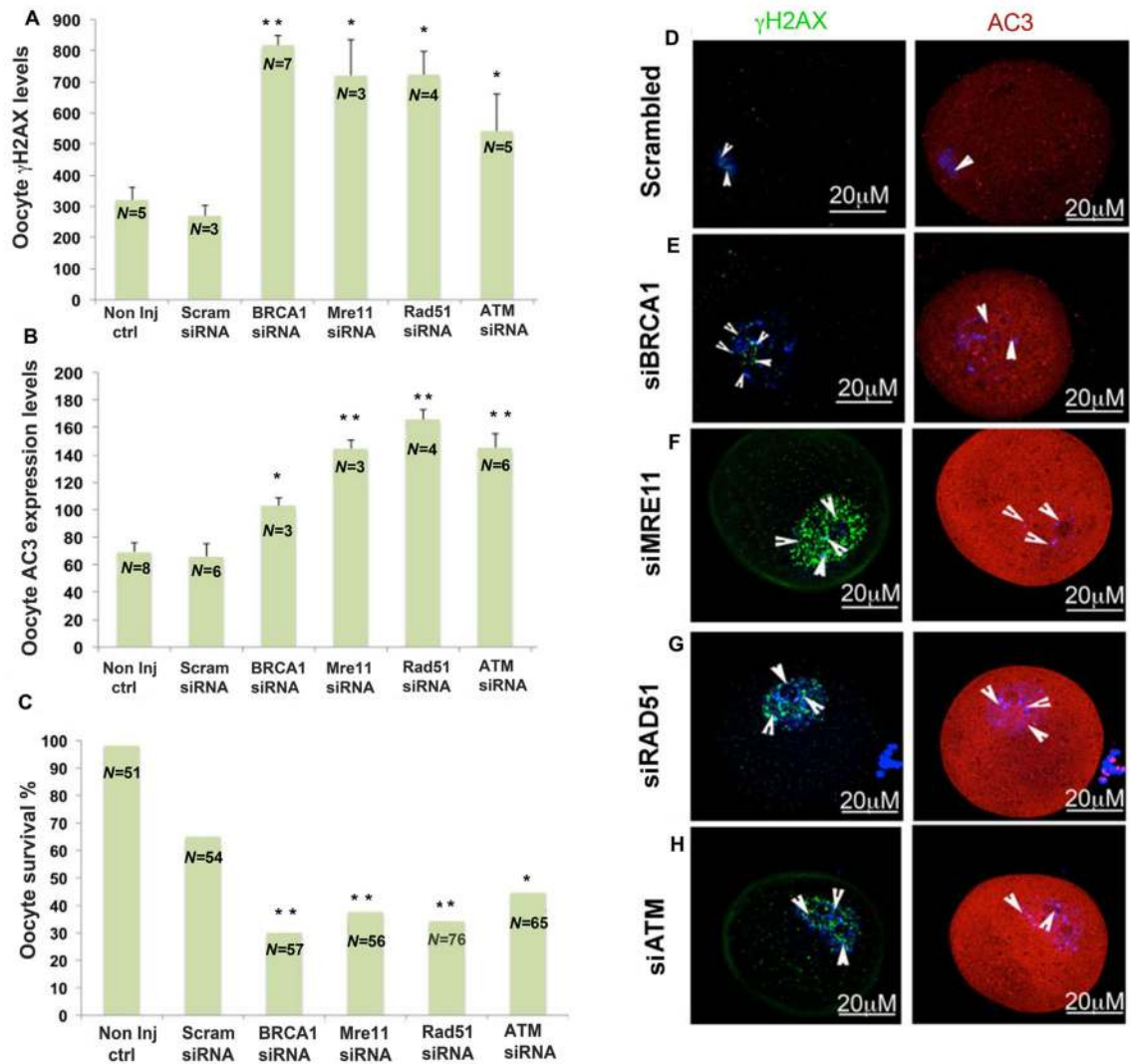


**Fig. 5. Impact of siRNA silencing of DNA repair genes on genomic integrity and survival of mouse oocytes in response to genotoxic stress**

In response to  $H_2O_2$  treatment (250  $\mu$ M) (**A**) mean number of  $\gamma$ H2AX foci increased ( $P < 0.05$ ; Student's  $t$  test) and (**B**) AC3 levels increased ( $P < 0.05$ ; Student's  $t$  test), whereas (**C**) survival decreased in the oocytes in which expression of DNA repair genes had been silenced compared to controls (scrambled siRNA) (Scram) ( $P < 0.05$  Fisher's exact test). Photomicrographs are representative of the  $\gamma$ H2AX foci (green) and AC3 (red) levels in the siRNA-silenced oocytes: (**D**) scrambled, (**E**) *BRCA1*, (**F**) *MRE11*, (**G**) *RAD51*, (**H**) *ATM*. All bar graphs show the mean  $\pm$  S.E.M. Arrowheads shows nuclear region. Oocytes are counterstained with DAPI (blue). non inj ctrl, noninjected control oocytes.



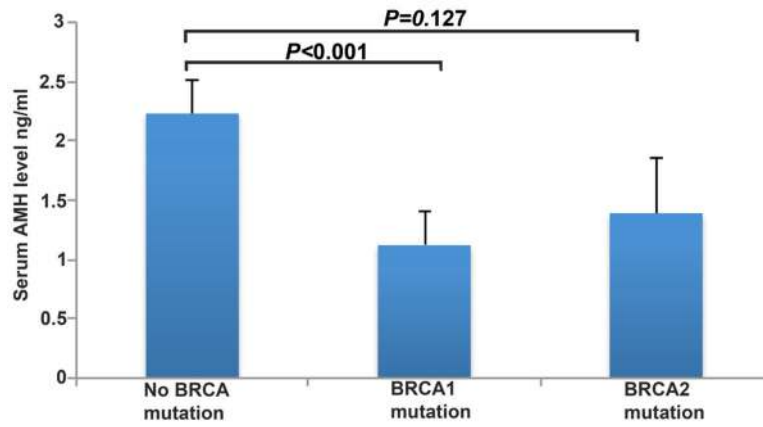


**Fig. 6. Diminished ovarian reserve in *BRCA1*-deficient individuals**

Women with significant *BRCA1* ( $P < 0.0001$ ; analyzed by ANOVA) but not *BRCA2* ( $P = 0.127$ ; analyzed by ANOVA) mutations had lower mean serum AMH concentrations compared to those with no *BRCA* mutations. All bar graphs show the mean  $\pm$  S.E.M.